Quaternary Science Reviews 30 (2011) 1112–1121

Contents lists available at ScienceDirect

Quaternary Science Reviews

journal homepage: www.elsevier.com/locate/quascirev

High-resolution opal records from the eastern tropical Pacific provide evidence for silicic acid leakage from HNLC regions during glacial periods

Elsa Arellano-Torres*, Laetitia E. Pichevin, Raja S. Ganeshram

School of Geosciences, University of Edinburgh, Grant Institute, West Main Road, EH9 3JW Edinburgh, UK

ARTICLE INFO

Article history:
Received 8 April 2010
Received in revised form
3 February 2011
Accepted 7 February 2011
Available online 8 April 2011

Keywords:
Opal
Silicic acid
Eastern tropical Pacific
Productivity
Last glacial
Carbon dioxide

ABSTRACT

A shift from carbonate- to silica-dominated primary production could significantly affect the oceanic carbon cycle via changes in the particulate carbon rain-rate ratio ($C_{organic}$:$C_{inorganic}$ fluxes). An increase in C rain rate ratio has been invoked to explain lower glacial pCO_2; however, firm evidence of an ecological shift towards silica-dominated productivity during the last glacial period is lacking. Here, we present new high-resolution reconstructions of biogenic silica and total production over the past 40,000 yr BP in 3 cores from the eastern tropical North Pacific (ETNP) off Mexico and Nicaragua. These records reveal a clear regional pattern of higher siliceous productivity with higher opal accumulation during the last glacial period compared to interglacial times. Higher Si:C and Si:N ratios of glacial sediments in these records suggest a net increase in siliceous production over total production. We attribute this to the additional supply of silicic acid to the ETNP margins favouring diatoms over other non-siliceous algae. This suggestion for increased supply of Si during glacial periods is consistent with the proposed large-scale redistribution of excess silicic acid from High Nitrate Low Chlorophyll (HNLC) regions like the eastern equatorial Pacific (EEP) and the Southern Ocean by the Silicic Acid Leakage Hypothesis (SALH). In these HNLC regions, the Si-isotope composition of diatom frustules ($\delta^{30}Si$) has provided evidence for the generation of surplus of silicic acid during diatom growth under conditions of higher Fe availability during glacial periods. We suggest that silicic acid leakage from the HNLC regions to the adjoining oceans may have increased the carbon rain rate ratio and ultimately, contributed to the decrease in glacial atmospheric pCO_2.

1. Introduction

Increase in the magnitude and changes in the nature of the marine productivity may have caused glacial declines in atmospheric CO_2 (pCO_2) (Berger and Wefer, 1991; Broecker et al., 1992; Archer et al., 2000a, 2000b). Model results suggest that a 40% increase in the *rain-rate ratio* (the flux of POC:$CaCO_3$ to the ocean interior) could explain the ~80 ppmv decrease in pCO_2 during the Last Glacial Maximum (LGM) relative to pre-industrial levels (Archer and Maierreimer, 1994; Ridgwell et al., 2002). However, such a severe change requires a drastic ecological shift in favour of non-calcareous phytoplankton like diatoms (Archer et al., 2000a). Such a shift could be caused by increasing the availability of silicic acid ($Si(OH)_4$) during glacial periods, permitting siliceous diatoms to out-compete smaller non-siliceous species such as calcareous coccolithophorids for limiting nutrients like nitrate (NO_3) and iron (Fe) (Ridgwell et al., 2002). The resulting enhancement in rain-rate ratios would in turn, decrease the alkalinity gradient between surface and deep-ocean lowering pCO_2 levels (Dymond and Lyle, 1985; Sigman and Boyle, 2000). Models of silica-dominated primary production causing lower glacial pCO_2 are also attractive because diatom frustules can transfer carbon to the deep-ocean more efficiently than pico- and nanoplankton, which are more prone to grazing pressure (Brzezinski et al., 2002; Ganeshram, 2002; Matsumoto et al., 2002).

1.1. Silicic acid availability and opal burial

Production of siliceous phytoplankton in large parts of the modern ocean is limited by the availability of silicic acid ($Si(OH)_4$) (Brzezinski and Nelson, 1996). The *Silicic Acid Leakage Hypothesis* (SALH) (Brzezinski et al., 2002; Matsumoto et al., 2002; Matsumoto and Sarmiento, 2008) postulates that a meridional redistribution of nutrients -rather than a whole-ocean increase in $Si(OH)_4$- could have promoted diatom production and increased the C rain rate

* Corresponding author. Tel.: +44 131 650 5980; fax: +44 131 668 3184.
E-mail addresses: e.arellano-torres@ed-alumni.net (E. Arellano-Torres), laetitia.pichevin@ed.ac.uk (L.E. Pichevin), raja.ganeshram@ed.ac.uk (R.S. Ganeshram).

0277-3791/$ – see front matter © 2011 Elsevier Ltd. All rights reserved.
doi:10.1016/j.quascirev.2011.02.002

ratios in low latitudes. This hypothesis stems from modern observations that High Nitrate Low Chlorophyll (HNLC) regions, where biological production is subject to severe Fe-limitation (e.g. the equatorial Pacific and the Southern Ocean), are also important areas of opal burial accounting for as much as two thirds of the Si sink in the modern ocean (DeMaster, 2002). The high opal burial in these HNLC regions is at least partly attributed to the production of heavily silicified diatom frustules under conditions of persistent Fe-limitation (Leynaert et al., 2004; Takeda et al., 2006). Thus, an increase in iron fluxes to HNLC regions during LGM might have relaxed Fe-limitation leading to a decrease in the relative utilisation of $Si(OH)_4$ compared to NO_3^- by diatoms. This conservation of $Si(OH)_4$ during diatom growth under Fe-replete conditions is supported by laboratory and shipboard bottle experiments (Martin et al., 1990; Takeda, 1998; Frank et al., 2000a; Marchetti et al., 2010), by artificial and natural Fe-fertilization (Nelson et al., 2001; Wong et al., 2006; Brzezinski et al., 2008; Mosseri et al., 2008), and by modelling studies in these areas (Takeda et al., 2006). In the Southern Ocean and equatorial Pacific, Fe-addition can account for a large decline in the Si:N uptake ratio, from ratios of ~4 to 1 to 1:1 (Takeda, 1998; Brzezinski et al., 2003; Marchetti and Cassar, 2009). The exact cause for this change in Si:N uptake ratios is currently being debated. The factors responsible may include reduced silicification of diatom frustules (Boyle, 1998; Takeda, 1998; Franck et al., 2000), differences in growth conditions, shifts in diatoms species composition and genetic variability or morphological changes (Marchetti and Cassar, 2009). Nevertheless, an important point to note is that a generally consistent outcome of iron fertilisation experiments in HNLC regions is the relative depletion of NO_3, leaving a surplus of $Si(OH)_4$. This surplus could be then transported out of these regions increasing diatom production in areas outside the HNLC region where $Si(OH)_4$ is limiting (Matsumoto et al., 2002; Pichevin et al., 2009).

Si-isotope composition ($\delta^{30}Si$) of diatom frustules has provided evidence for the presence of surplus $Si(OH)_4$ during the LGM in the Southern Ocean (Brzezinski et al., 2002) and the eastern equatorial Pacific (EEP) (Pichevin et al., 2009). However, glacial–interglacial trends in opal accumulation over large region such as the Southern Ocean could be variable, perhaps responding to additional local factors such as sea ice cover, stratification and wind mixing, or sediment redistribution (Francois et al., 1997; Dezileau et al., 2003; Bradtmiller et al., 2009). Therefore, it is critical to evaluate further the evidences for the conservation and redistribution of silicic acid during diatom growth in the glacial ocean under increased Fe-availability. An important aspect of this evaluation is to assess whether the excess silicic acid exported out of the HNLC regions acted as a net additional source of $Si(OH)_4$ for adjoining areas. Importantly, this additional $Si(OH)_4$ source could have drastically increased diatom growth in the glacial ocean in areas where Si is in short supply allowing diatoms to out-compete calcareous algae and leading to a net increase in the C rain rate ratio (Matsumoto and Sarmiento, 2008).

In this study, we investigate the evidence for increased $Si(OH)_4$ supply to the eastern tropical North Pacific (ETNP) margins (Fig. 1). We present 3 high-resolution records of opal contents (wt %), Si:C and Si:N ratios, spanning the last 40,000 yrs. The ETNP margins are well suited to evaluate the export of excess silicic acid from HNLC regions during glacial periods for the following reasons. First, productivity in these upwelling margins is limited by availability of Si and N, but not generally constrained by persistent Fe limitation (Fig. 1). Second, the generation of excess $Si(OH)_4$ in the glacial Southern Ocean and the EEP should augment Si supply to the ETNP margins due to regional surface and subsurface circulation of the eastern Pacific. Therefore, diatom production in ETNP margins is expected to respond sensitively to the excess silicic acid supply from HNLC regions during glacial periods.

2. Study site and methods

Three marine sediment cores were retrieved from the eastern tropical North Pacific (ETNP) with a Calypso piston corer during the MONA Cruise (IMAGES VIII-Internal Marine Global Changes, Jun-2002) (Fig. 1). The Core MD02-2519 was collected off Mazatlan, NW Mexico (lat. 22°30.89'N; long. 106° 39.00'W; 955 m water depth); the Core MD02-2520 from the Gulf of Tehuantepec, Mexico (lat. 15°40.14'N; long. 95°18.00'W; 712 m water depth); and the Core MD02-2524 from the Nicaragua Margin (lat. 12°00.55'N; long. 87°54.83'W; 863 m water depth). The ETNP is a region of high-productivity and elevated chlorophyll-*a* concentrations (Fig. 1-A) fuelled by active seasonal upwelling of subsurface waters of equatorial origin (Kessler, 2006). The ETNP margins are generally characterised by low silicic acid concentrations (Fig. 1-B) where $Si(OH)_4$

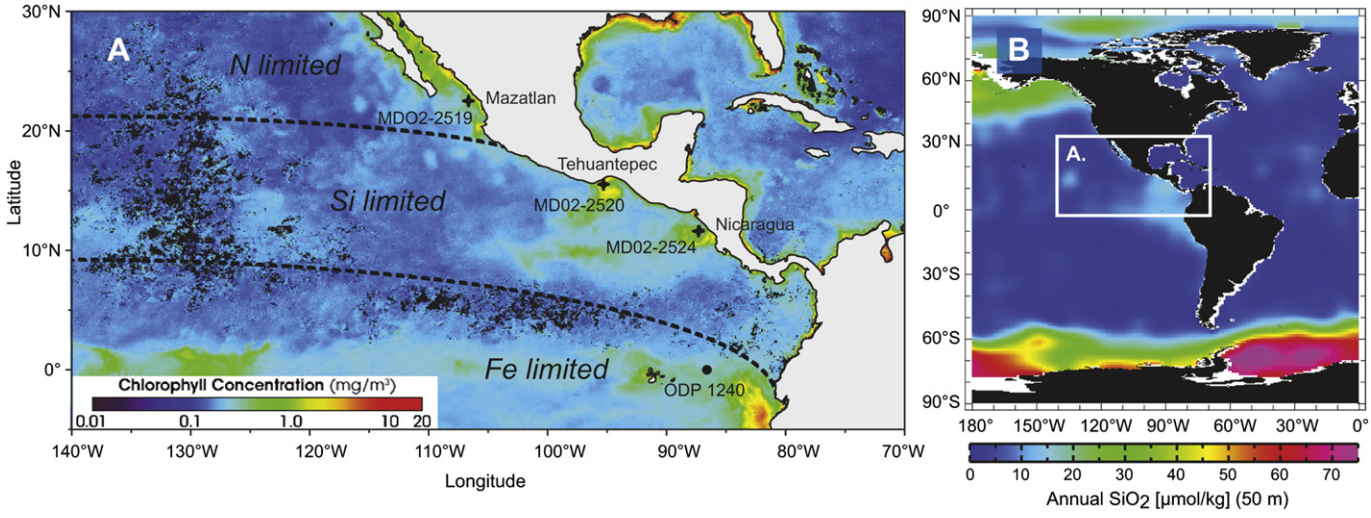

Fig. 1. Study area. (A) Location of cores collected off Mazatlan (MD02-2519), the Gulf of Tehuantepec (MD02-2520) and Nicaragua (MD02-2524). Core ODP 1240 collected north of the Carnegie Ridge in the Panama basin (0°01.31 N; 86°27.76 W; 2.921 m water depth) (Pichevin et al., 2009). Colours show the average Chlorophyll-*a* concentrations (mg/m^3) during winter derived from SeaWIFS satellite imagery. Dotted lines show areas of N, Si and Fe limitation in the eastern tropical Pacific (*from* Moore et al., 2004). (B) [SiO_2] at 50 m depth (Levitus et al., 1994).

commonly limit algal growth but persistent Fe limitation is absent (Pennington et al., 2006). This is in contrast with the equatorial divergence region of the EEP, where severe Fe followed by Si limitation prevail (Moore et al., 2004). The cores are located under the intense oxygen minimum zone in the ETNP, where denitrification causes a broad N-deficit at the subsurface of 26.5 isopycnal.

The sediment sequences from the cores MD02-2519, MD02-2520 and MD02-2524 are either massive or laminated, alternating with faintly bioturbated intervals that generally do not exceed more than 10 cm. The laminations range from fine (0.5–2 mm) to thicker banding (5–20 mm). These sediments mostly consist of silty-clay of olive-grey to dark olive-grey colour. Other minor lithologic components include layers and lenses of volcanic ashes. Notably, these cores are devoid of coarse sand layers, abrupt bending or oblique stratification that may indicate terrestrial inputs or lateral transport. Organic matter preserved in these sediments are overwhelmingly of marine algal origin and $\delta^{13}C$ values fall well with in the range for marine organic matter (i.e. -22 to -19‰) with down core variations in the order of ~1.5‰ (Pichevin et al., 2010). These results are also consistent with previous studies in this area (Ganeshram et al., 1999).

Geochemical analyses of C, N and biogenic Si (Si_{OPAL}) were performed in specialised laboratories at the School of Geosciences, The University of Edinburgh. After sub-sampling the sediment cores for every 2 cm, the samples were freeze-died, ground and homogenized using an agate mortar. The samples selected for C-N analyses were decalcified with HCl (5%) on a hot plate at 70 °C, and organic C and N were determined using a C-N Elemental Analyser (CE Instruments NA2500). Biogenic Si (Si_{OPAL}) determination were done at 5 to 10 cm resolution using molybdate-blue spectrophotometry after alkaline extraction (2N Na_2CO_3 solution at 85 °C for 3 h) following Mortlock and Froelich (1989). The opal (wt%) was calculated using the equation: %opal = Si_{OPAL} x *2.4*; where *2.4* is the *conversion factor* assuming that most of the diatomaceous silica (younger than 30 Ma) displays a relatively constant water mass of about 10% (formula: $SiO_2 \cdot 0.4H_2O$) (Mortlock and Froelich, 1989). The precision and accuracy of opal analysis were monitored using replication of two internal sediment standards (*a* and *b*), from sediments collected off Mazatlan and the Gulf of California. *STD-a* is the sample 0-1 cm of the Core MD02-2519 ($n = 35$; max = 4.39 wt%, min = 3.10 wt%; 1σ std dev. = 0.35). *STD-b* is a diatom-mud sample from the Gulf of California ($n = 35$; max = 40.14 wt%, min = 32.10 wt%; 1σ std dev. = 2.33). To calculate the Si_{OPAL}:C and Si_{OPAL}:N ratios (*hereinafter* Si:C and Si:N), the elemental composition of organic C and N (wt%) was transformed to molar ratios.

2.1. Age models and sedimentation rates

The age models of the cores are mostly based on accelerator mass spectrometry (AMS) radiocarbon dates (<45,000 cal yr BP). The AMS^{14}C dates were determined at the NERC Radiocarbon Laboratory, East Kilbride, Scotland, UK. The chronologies of the cores MD02-2519, MD02-2520 and MD02-2524 are based on 19, 29 and 19 AMS^{14}C dates (Fig. 2 and Fig. 3). The age model for Core MD02-2519 listed in Table 1, whereas the age models for cores MD02-2520 and MD02-2524 are reported in Pichevin et al. (2010). All AMS^{14}C dates were converted to calendar years before present (BP) using the online version CALIB 5.0.2 for marine samples (Stuiver et al., 2005). The local reservoir corrections (ΔR) correspond to 203 ± 48 yrs (MD02-2519), 162 ± 50 yrs (Core MD02-2520) and 281 ± 50 (Core MD02-2524), as reported in the Marine Reservoir Correction Database (Reimer and Reimer, 2001). Samples older than 21,800 ^{14}C yrs were calibrated with the polynomial equation by Bard et al. (2004).

Mass accumulation rates (mg/cm^2/ka) of the biogenic opal were calculated with the formula: MAR = [2400 (mg/cm^3)] [1 − porosity]

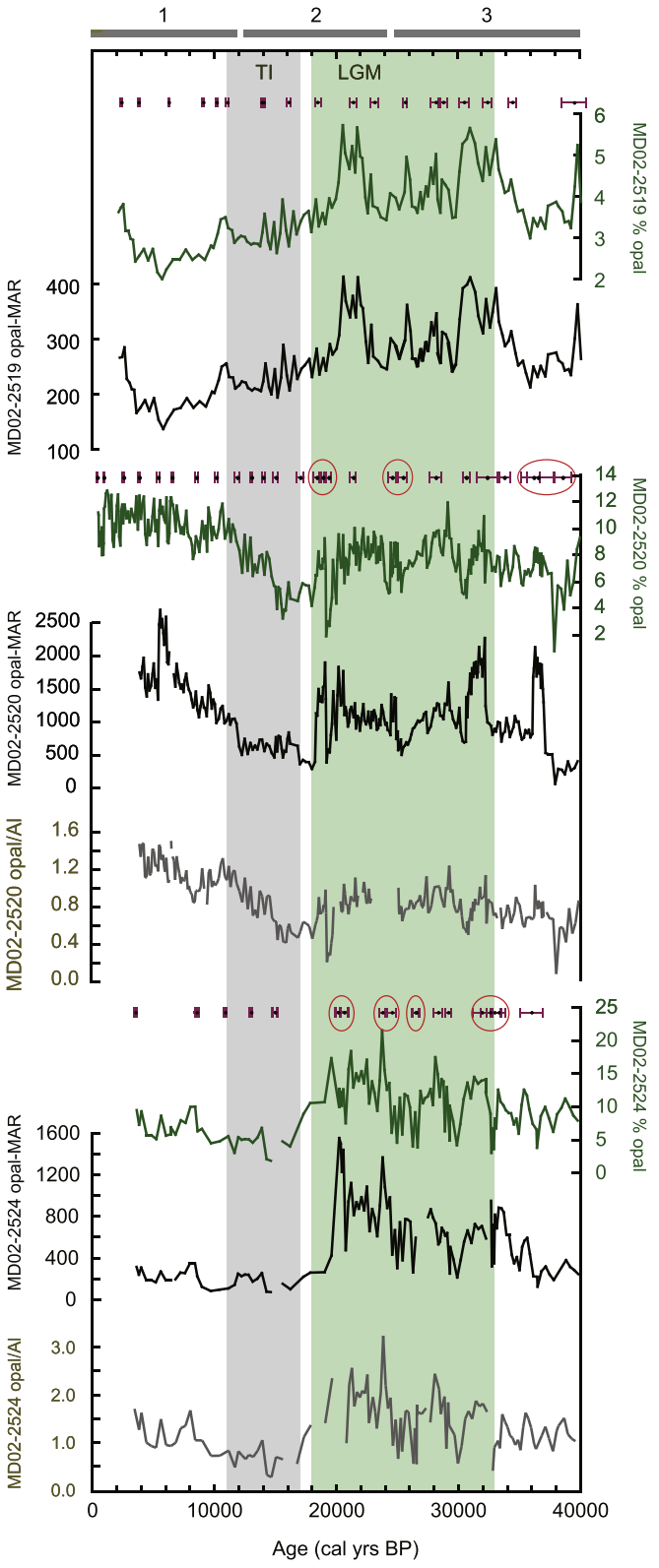

Fig. 2. (A) Comparisons between opal (wt %) and opal-MAR for each core taken from the ETNP; dots with error bars mark the position of AMS^{14}C dates; red circles show the pair dates that have been averaged to calculate opal-MAR. Numbers on top are Marine Isotope Stages (MIS) 1 to 3. The pale-green band highlights the period of opal maximum between 33,000 – 18,000 yrs, while the grey band the period of opal minimum between 17,000 -11,000 yrs. TI and LGM stand for Termination I and Last Glacial Maximum, respectively.

[SR (cm/ka)] [fraction of *organic carbon* or *opal*] (Ganeshram et al., 1995); where the value *2400* is the assumed grain density and *SR* is the sedimentation rate between control points. The porosity data were measured on board the ship (Beaufort, 2002). In Fig. 2 is shown the position of the AMS^{14}C dates, the average SR and the comparison between opal (wt%) and opal-MAR for the last 40,000 yrs. Averages of the SR were calculated for the cores MD02-2520 and MD02-2524 to avoid SR-artefacts caused by the proximity between radiocarbon dates (marked with red circles in Fig. 2). In addition, MAR estimates for the last 2000 yrs of Core MD02-2520 are not taken into account because of spurious fractional porosity data. For these reasons, the opal-MARs are only used to describe the patterns at glacial–interglacial timescale.

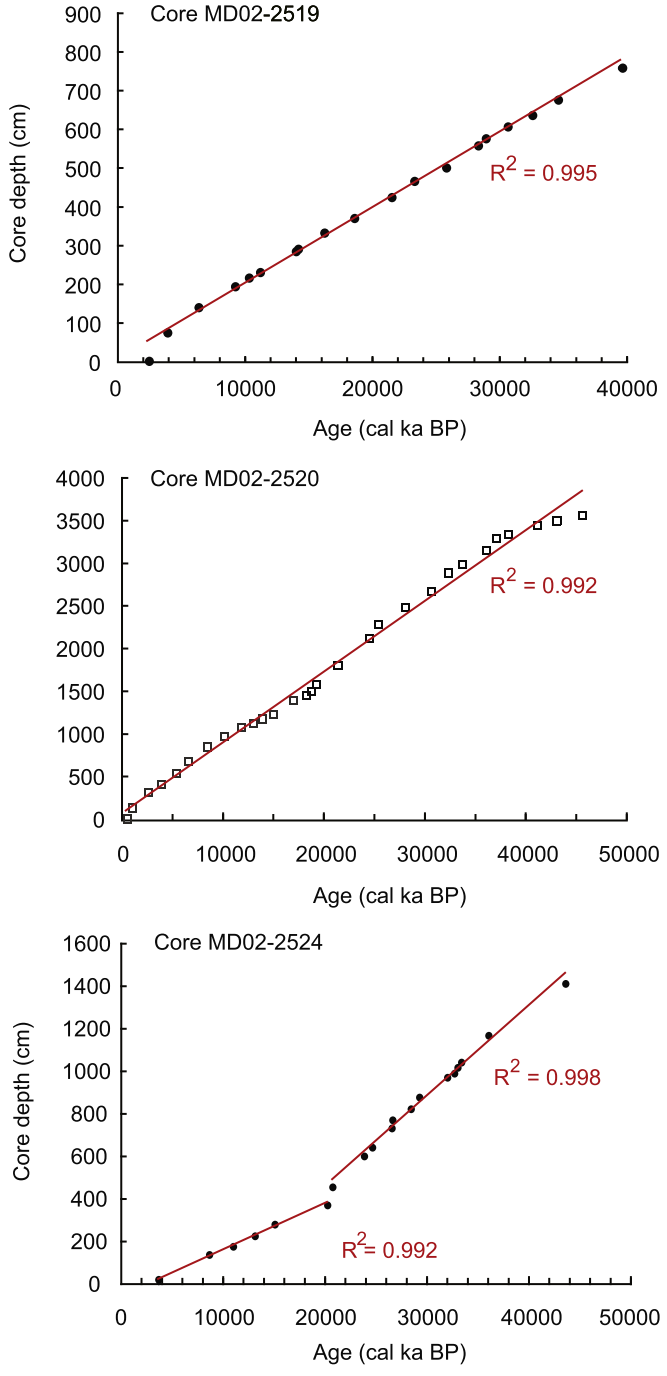

Fig. 3. Age models. AMS^{14}C dates vs. depth of the cores MD02-2519 (Mazatlan) (see Table 1), MD02-2520 (Tehuantepec) and MD02-2524 (Nicaragua) (Pichevin et al., 2010).

3. Results and discussion

3.1. Evaluating opal proxy records

The biogenic silica is measured as the opal concentration (wt%) in the sediments, and represents the relative contribution of opal producing organisms (mainly diatoms, but to a lesser extent radiolarians and possibly sponge spicules) to the total sediment (Egge and Aksnes, 1992; Ragueneau et al., 2000). In the continental margins, the sediment opal contents could be influenced by sediment redistribution, differential preservation during settling and burial, and dilution by other sedimentary components (Ragueneau et al., 2000; Nelson et al., 2001, 2002; DeMaster, 2002). Therefore, failure to recognize such influences can lead to misinterpretations of the sedimentary opal as a tracer of changes in productivity of siliceous plankton.

In this study, however, we interpret variations in opal contents as mainly reflecting surface opal production and fluxes of opal to the seabed, based on the following observations. In sediments from the continental margin (with shallow water column) most of the opal dissolution principally occurs at the sediment surface and in superficial sediments (Ragueneau et al., 2000). Therefore, opal preservation is normally expected to increase with higher sediment accumulation rate. However, we do not observe a systematic relationship between opal contents and sedimentation rate in our records (Fig. 2), where the broad glacial–interglacial variations are largely independent of sedimentation rates, which are linear in two of the three cores studied (Fig. 3). Thus we exclude differential preservation as the main factor influencing down core changes in opal contents. In addition, the Si:C and Si:N ratios broadly follow the pattern of %opal (as shown in Fig. 5), which reduces the importance of dilution by terrigenous inputs controlling variability in these records. To verify that the %opal records are not being

Table 1
Radiocarbon dates of Core MD02-2519.

	AMS 14C dates: Core MD02-2519							
	Core depth	Raw ^{14}C Age	error	Calibrated Age	error 1σ		Notes:	
	(cm)	(yrs)	±	(yrs BP)*	−	+	material	data source
1	1	2865	73	2365	116	94	OC	1
2	74	4049	61	3802	79	93	OC	1
3	140	6050	61	6266	54	72	OC	1
4	194	8689	64	9114	79	101	OC	1
5	216	9555	73	10198	82	84	PF	1
6	230	10272	62	11082	134	94	PF	1
7	284	12664	53	13911	86	75	OC	1
8	290	12831	64	14084	84	76	PF	1
9	332	14173	65	16139	205	193	PF	1
10	370	15717	84	18475	184	296	OC	1
11	424	18667	109	21417	278	272	OC	1
12	466	20091	173	23191	316	346	OC	1
13	500	21920	153	25713	208	145	OC	1
14	558	24147	154	28226	399	399	OC	2
15	576	24690	169	28831	369	369	OC	2
16	606	26239	216	30548	364	364	OC	2
17	636	27987	281	32471	349	349	OC	2
18	676	29852	367	34507	342	342	OC	2
19	758	35012	749	39522	1015	1015	OC	2

OC - organic carbon; PF – planktonic foraminifera.
(1) Stuiver *et al.*, 2005; (2) Bard et al., 2004.
* $\Delta R = 203 \pm 48$.

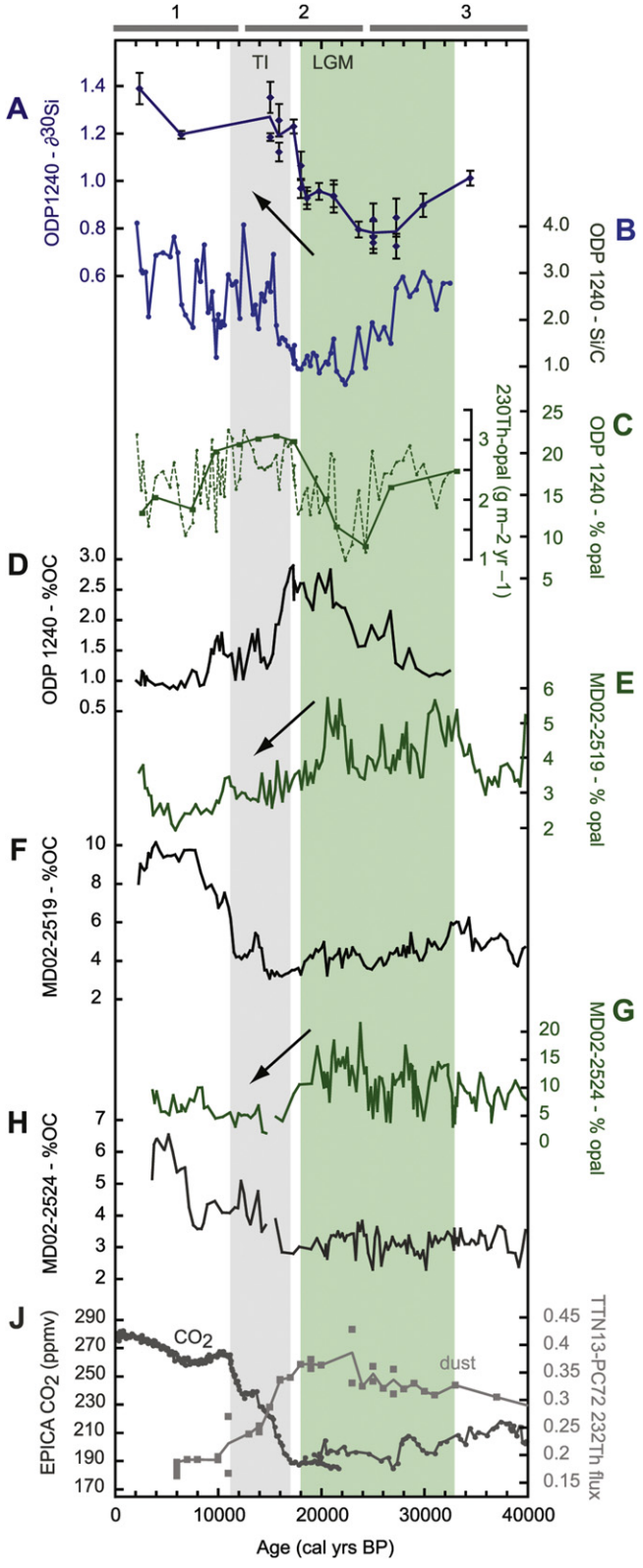

Fig. 4. Opal and organic carbon records of cores collected from the EEP and ETNP plotted vs. calendar ages BP (shown in green and black lines respectively). Numbers on top are MIS 1 to 3. Core ODP 1240 (Eastern Equatorial Pacific) records (Pichevin et al., 2009) of (A) δ^{30}Si of diatoms, (B) Si:C ratio, (C) opal (wt% - dotted line) and ^{230}Th normalized accumulation rates (solid line), and (D) organic carbon (OC wt%). Core MD02-2519 (Mazatlan) records of (E) % opal and (F) % OC. Core MD02-2524 (Nicaragua) records of (G) % opal; (H) % OC. EPICA Dome C records of (I) dust flux (^{232}Th flux – μg/cm^2/ka) linked to Fe input in the central equatorial Pacific (Winckler et al., 2008); (J) atmospheric CO_2 concentration (ppmv) (Monnin et al., 2001; Ahn and Brook, 2008) showing the ~80 ppmv change from LGM to the Holocene. Black arrows show the trend of glacial to interglacial biogenic Si change. TI – Termination I, and LGM – Last Glacial Maximum.

biased by dilution by other non-terrigenous inputs, such as $CaCO_3$, opal/Aluminium ratios were calculated in the cores MD02-2420 and MD02-2524 from existing Al data (by S. Francavilla (*unpublished data)* and Pichevin et al. (2010), respectively). The opal/Al ratios plotted in Fig. 2, show trends that are largely similar to %opal records confirming that differential dilution by non-terrigenous inputs is not causing the variability in %opal records. These interpretations are also supported by the broad agreements between opal-MAR and %opal records, with a few exceptions. For instance, the regional opal pattern seen in our 3 records (i.e. increased opal contents during the last glacial and its decline starting at 18,000 yrs – Fig. 2) cannot be simply explained by site-specific processes such as sediment redistribution and focussing, given that these processes are expected to vary from one site to the other. Therefore, in this study we treat %opal changes reflecting variations in opal supply to the sediments from the upper water column in a more qualitative sense.

3.2. Glacial–interglacial opal variations

The opal records (i.e. %opal and opal-MARs) form ETNP cores over the last glacial-interglacial (G-IG) cycle are shown in Fig. 2. All ETNP records show relatively consistent trends where the opal content is higher between 33,000 and 18,000 yrs, with maximum values during the Last Glacial Maximum (LGM; 24,000–19,000 yrs). The most pronounced %opal change in the ETNP cores is the drastic decline at about 18,000 yr. For instance, at the end of the LGM and over Termination I (18,000–11,000 yrs) the %opal record from off Mazatlan (Core MD02-2519) declined from maximum values of ~6% to minimum values of 2%. Off Tehuantepec (Core MD02-2520), the %opal changed from 10% to 3%; whereas off Nicaragua (Core MD02-2524) it changed from ~18%–2%. The opal-MARs confirm this pattern at glacial–interglacial timescales in all records (Fig. 2). The Nicaragua and Mazatlan records show low %opal (i.e. < 3.5% and <9%, respectively) during the Holocene. Such low Holocene values have been also reported previously in records from the Gulf of California (Douglas et al., 2007), Therefore, the trend towards low opal contents during the Holocene relative to the glacial seems to be widespread in this margin. The exception is the opal record from the Gulf of Tehuantepec. Here, the opal contents decline during T1 like in the other ETNP records, but recovers rapidly to values higher than 10% during the Holocene (Fig. 2). This unusual pattern of high Holocene opal contents appears to be unique to the Gulf of Tehuantepec and will be discussed separately (thus not included in Fig. 4). Moderate opal contents prevail during MIS 3 (>24,000 yrs) relative to the high values during the LGM (24,000–19,000 yrs).

A prominent feature in all ETNP opal records is the drastic decline in opal contents and accumulation rates during TI following maximum values during LGM. This pronounced decline in opal content and accumulation rates after 18,000 yr (Fig. 2, and Fig. 4), could be explained by a decrease in upwelling and productivity in the ETNP margins at the end of last glacial period. The organic carbon (OC) record presented show a glacial–interglacial pattern that is different from opal where OC contents drastically declines during the last glacial period (Fig. 5-F & H). Such glacial to Holocene increase in OC has been previously suggested as an evidence for increased upwelling and productivity at the end of the last glacial period and have been replicated in a range of productivity proxies including biogenic barium, %$CaCO_3$, planktonic ^{13}C and surface dwelling foraminifera abundances (Ganeshram and Pedersen,

1998; Hendy and Kennett, 2000; Hendy et al., 2004; Ortiz et al., 2004). These studies exclude differential OC preservation as the main cause for glacial to interglacial increases in OC contents (Ganeshram et al., 1999). In fact, the glacial decline in upwelling and productivity suggested by OC records is a regional trend that extends over much of the western American margin (Hendy and Kennett, 2000; Hendy et al., 2002, 2004; Barron et al., 2004; Ortiz et al., 2004). Thus the declining trends in opal records during the last termination require an alternative explanation.

As shown in Fig. 5, the Si:C and Si:N ratios generally follow opal contents with high values between 33,000 and 18,000 yrs, indicating that opal production (as a proportion of total productivity)

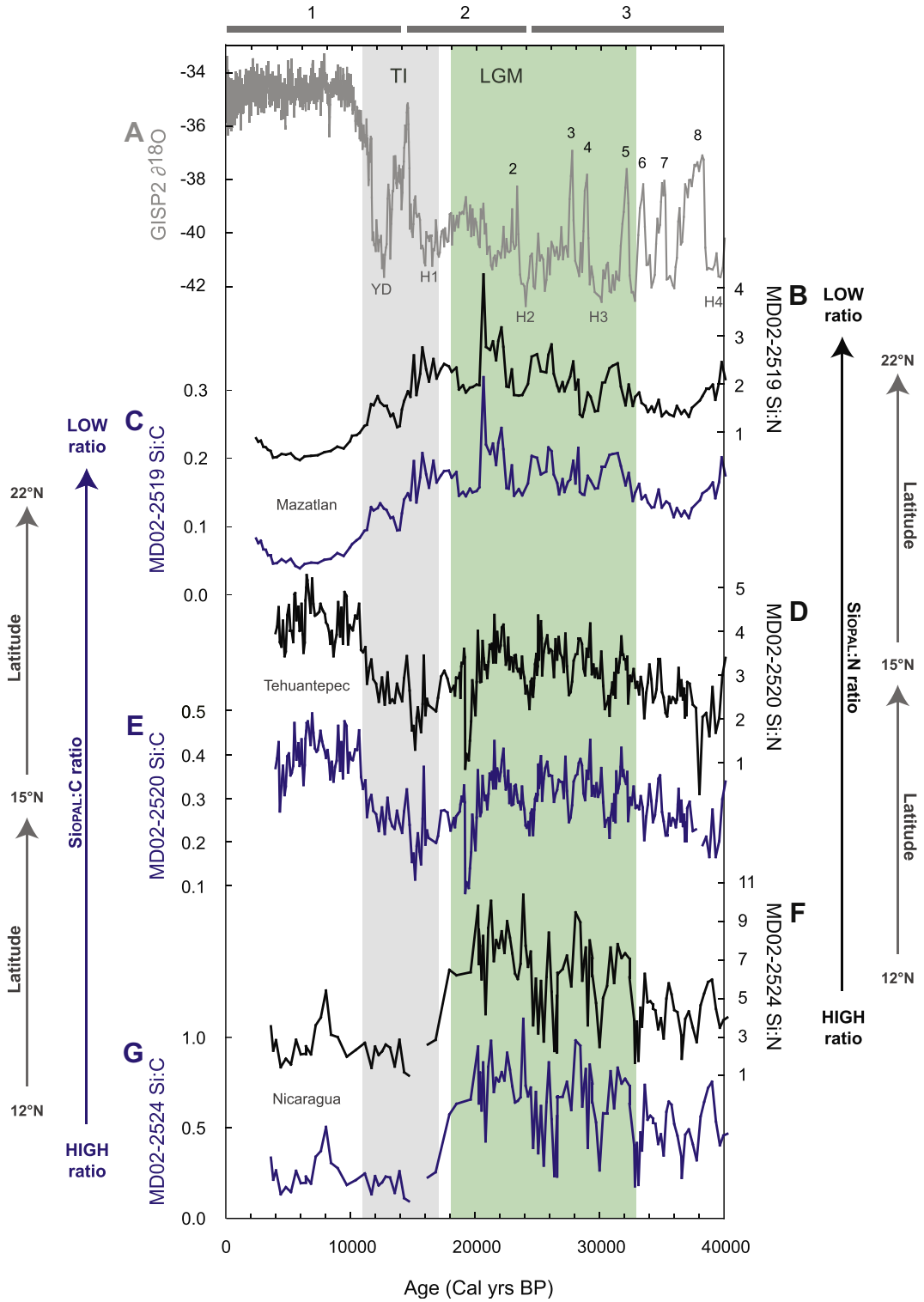

Fig. 5. Molar Si_{OPAL}:C and Si_{OPAL}:N ratios of cores collected from the ETNP. (A) GISP2 $\delta^{18}O$ record used for reference. (B and C) Core MD02-2519 (Mazatlan); (D and E) Core MD02-2520 (Tehuantepec); (F and G) MD02-2524 (Nicaragua). Arrows indicate the decrease in Si_{OPAL}:C and Si_{OPAL}:N ratio with increase in latitude.

Table 2
Average Si:C and Si:N M ratios of cores MD02-2519, MD02-2520 and MD02-2524 over Marine Isotope Stages 1 to 3.

	Si/C	Si/N
	MIS-1	
MD02-2519	0.07	0.87
MD02-2520	0.36	3.87
MD02-2524	0.23	2.49
	MIS-2	
MD02-2519	0.17	2.20
MD02-2520	0.28	3.02
MD02-2524	0.64	6.38
	MIS-3	
MD02-2519	0.14	1.69
MD02-2520	0.28	2.79
MD02-2524	0.48	4.56

increased during this period and subsequently declined during the onset the last interglacial (*see* Table 2). In all records, the Si:C and Si:N M ratios exhibit a 2.4 to 2.8–fold declines from the LGM to TI. Therefore the higher glacial Si:C and Si:N ratios can be the result of a shift in the type of production. For instance, a shift away from the dominance of diatoms to non-siliceous algae at the end of LGM could explain the declining trends Si:C and Si:N ratios during the last termination. In the following paragraphs this hypothesis is further addressed by exploring the role of possible changes in supply of silicic acid during the last glacial-interglacial cycle.

In contrast with the ETNP, the eastern equatorial Pacific (EEP) sediment exhibit an opal minimum during the LGM relative to the Holocene, and a gradual increase during T1(Fig. 4–C). This pattern of LGM decline in opal fluxes has been reproduced in other sites in the EEP (e.g. Bradtmiller et al., 2006; Kienast et al., 2006; Pichevin et al., 2009) leading to the suggestion that opal burial declined as a whole in this region during the LGM by a factor of 1.3 (Pichevin et al., 2009). The LGM minimum in Si:C ratios seen in Core ODP-1240 is also typical of many EEP records (Fig. 4–B). A recent study investigated the cause for glacial–interglacial change in opal burial in the EEP, and showed that the glacial decline in opal burial is matched by the lighter excursion of Si-isotopes (Fig. 4–A) recording excess unutilised $Si(OH)_4$ in the surface waters of the EEP. This condition was attributed to enhanced Fe inputs to the EEP during LGM either by increased dust flux (Fig. 4–I) (McGee et al., 2007, Winckler et al., 2008) and potentially through upwelling (Lefevre and Watson, 1999; Watson et al., 2000).The increased Fe supply during the glacial could then lower Si utilisation compared to other nutrients, resulting in reduced opal fluxes and burial. This study hypothesized that the excess $Si(OH)_4$ thus generated in the EEP during glacial periods, could furnish an additional source of $Si(OH)_4$ to adjoining Si-limited regions such as the ETNP during this time contributing to the glacial CO_2 drawdown recorded in ice cores (Fig. 4–J). Similarly, silicic acid supply to the low latitudes from the glacial Southern Ocean has also been previously envisioned by the SALH (Brzezinski et al., 2002; Matsumoto et al., 2002). Although glacial–interglacial change in opal burial in the Southern Ocean could be variable, influenced by a range of local factors, the LGM decrease in opal burial has been reported in the Pacific sector of the Southern Ocean (Frank et al., 2000b; Chase et al., 2003; Diekmann, 2007). Therefore, if the glacial ETNP was a recipient of this additional supply of $Si(OH)_4$ from the HNLC regions, this would have favoured diatom production over non-siliceous production. The increased opal burial, and the high Si:C and Si:N ratios recorded in the ETNP cores during the LGM, and the subsequent decline in these parameters during TI (after 18,000 yrs) is consistent with excess silicic acid supply from the EEP and possibly from the Southern Ocean during glacial periods (Figs. 4 and 5). This conclusion is also consistent with recent suggestions that Si mass balance in the LGM ocean demands a hitherto unidentified additional sink of Si -perhaps in the margins- to compensate for the decline in Fe burial in HNLC regions during glacials (Bradtmiller et al., 2009).

3.3. Silicic acid leakage during the last glacial period

Several lines of evidence support the contention that the glacial ETNP may have received excess $Si(OH)_4$ from HNLC regions such as the EEP, leading to an increase in siliceous production. First, continental margins bordering the ETNP are particularly sensitive to additional export of silicic acid because the biological productivity in these margins is either Si- or N-limited (Fig. 1), but not severely Fe-limited – a condition that occurs only transiently at the end of upwelling episodes in restricted localities (Firme et al., 2003; Moore et al., 2004; Pennington et al., 2006). The absence of severe Fe-limitation is evident from the rapid depletion of macronutrients by biological utilisation in upwelled waters along the coast (Hutchins and Bruland, 1998; Bruland et al., 2001). Thus, any additional supply of $Si(OH)_4$ during the last glacial period is expected to favour diatom production over other non-siliceous algae increasing opal production along the ETNP margins. Second, subsurface waters of the ETNP are fed by waters sourced from the South Pacific via the equatorial region furnishing a pathway of excess $Si(OH)_4$ from the EEP and the Southern Ocean to reach our study sites. Pivotal to this pathway is the Equatorial Undercurrent (EUC) which originates in the western Pacific, largely from SubAntarctic Mode Water (SAMW), North Equatorial Countercurrent (NECC) and New Guinea Coastal Undercurrent (NGCUC) (Toggweiler and Carson, 1995; Dugdale et al., 2002). As the EUC flows eastward along the equator, it is modified through mixing with zonal currents such as the South Equatorial Current (SEC), the Subtropical Mode Water (STMW), and through gaining heat and salt together with the Tsuchiya jets (abbreviated NSSCC and SSSCC) (Tsuchiya and Talley, 1996, 1998). In the EEP, these modified waters are partly transformed into Subtropical Subsurface Water (SSW) that flows along the ETNP margin and is tapped to the surface along the eastern Pacific by wind forcing and coastal upwelling (Wyrtki, 1966; Kessler, 2006). Furthermore, the mixing of zonal currents with the EUC leads to exchange at the surface waters as they travel north via the Costa Rica Coastal Current (CRCC) and the Western Mexican Current (WMC) (Fiedler and Talley, 2006; Kessler, 2006).

In the modern ocean, the water sourced from the South such as the NGCUC and the lower EUC (250–350 m depth) is low in Si relative to N compared to waters sourced from the North such as the NECC. This low nutrient ratios in subsurface waters sourced from the South are consistent with Fe limitation and extraction of silicic acid in higher proportion in the Southern Ocean (Dugdale et al., 2002). However, the generation of excess $Si(OH)_4$ in the Southern Ocean should have drastically altered the nutrients ratios of water sourced from the South to the EEP during the glacials. The Mode Waters particularly furnish a pathway for meridional transport of excess $Si(OH)_4$ from the Southern Ocean to the tropics (Matsumoto et al., 2002), which could then be fortified further with excess silicic acid in the EEP (Bradtmiller et al., 2009; Pichevin et al., 2009) and advected to the ETNP through surface and subsurface circulation.

The high opal content and accumulation rate during the last glacial period, as well as the pronounced decline in opal content and accumulation rate after 18,000 yr (Fig. 4), appears to be common occurrences in the opal records along the eastern Pacific margins in both hemispheres, where equatorial waters upwell to the surface (Kessler, 2006). Off Peru and Chile (24°S - 33°S),

increased opal burial during the LGM relative to the Holocene has been previously reported (Mohtadi and Hebbeln, 2004).

The northward transfer of excess $Si(OH)_4$ via the EEP to the ETNP during the last glacial is also supported by the gradients in opal contents exhibited by the glacial ETNP sediments. Marginal sites closer to the equator (i.e. Nicaragua) have higher opal values during the LGM than the record from farther north (i.e. Mazatlan) (Fig. 4). Furthermore, the Si:C and Si:N ratios decrease with increasing latitude (Fig. 5). The core from Nicaragua shows the highest average Si:C and Si:*N* values during the glacial (0.6 and 6.0, respectively), followed by the core from the Gulf of Tehuantepec (0.3 and 3.0, respectively), then the northernmost core from Mazatlan (0.15 and 2.0, respectively). This gradient may suggest that the Si:C and Si:N ratios are broadly tracing the northward pathway followed by surface and subsurface currents along the ETNP margin, and the gradual decline in Si export towards the north due to biological consumption.

3.4. Holocene differences between opal records

During the mid- to late Holocene (<11,000 yrs), the core collected from the Gulf of Tehuantepec shows high opal contents, which differs from the lower values seen in the cores taken off Mazatlan (MD02-2519) and Nicaragua (MD02-2524) (*compare* Figs. 2 and 5). We attribute this unique Holocene feature to local factors that lead to elevated mid- to late Holocene opal contents in the Gulf of Tehuantepec sediments. We also note that this elevated Holocene %opal contents are matched by higher Si:C and Si:N ratios (Fig. 5), indicating that this may have been the result of increased opal production as a proportion of total production, perhaps linked to an additional source of $Si(OH)_4$ established after ~11,000 yrs.

Today, the upwelling of the Gulf of Tehuantepec is one of the most prominent features along the ETNP margin (Fig. 1). The area experiences extremely high biological production, where two important wind-forcing events of mesoscale variability (i.e. length scale of $\sim 10^2$ km) occur annually. The most significant wind-driven events (called *Tehuanos*) occur during winter-spring resulting in intense upwelling that supplies large amounts of nutrients to the euphotic zone (Trasviña et al., 1995; Barton et al., 2009), a condition that is common in the eastern boundary currents regimes of the ETNP margins (Kessler, 2006). The second event, unique to the Gulf of Tehuantepec, occurs during summer when the cross-isthmus wind-jet induces dipole eddy formation (Trasviña and Barton, 2008) leading nutritive waters from ~100 m depth to reach the photic zone as a result of the cyclonic circulation (Farber-Lorda et al., 2004; Barton et al., 2009). As a consequence, the Gulf of Tehuantepec experiences elevated chlorophyll-*a* concentrations ([Chl-a] ~3–5 mg/m^3) and the highest annual average supply of silicic acid to the euphotic zone (i.e. $[SiO_2]$ ~42.5 μM; mean concentrations between 0 − 100 m water depth) which is more than double of what other areas in the ETNP receive on annual basis. For instance, the annual average $[SiO_2]$ in the coastal boundary current regions are ~19.7 μM off Mazatlan and ~16.8 μM in the Gulf of Papagayo (Pennington et al., 2006). In contrast, the annual average nitrate concentration in the euphotic zone does not show such an anomaly in the Gulf of Tehuantepec. Along the ETNP margin, the nitrate is gradually exhausted northward of the equator as a consequence of denitrification, which consumes nitrate in the upwelling source waters (Moore et al., 2004; Pennington et al., 2006). For example, the annual average $[NO_3^-]$ ~20.3 μM in the Gulf of Papagayo, ~18.3 μM in the Gulf of Tehuantepec and ~14.0 μM off Mazatlan. Thus in the Gulf of Tehuantepec, the $[SiO_2]$ to $[NO_3^-]$ ratios of upwelled waters are at least twice as high as other areas in the ETNP, which is attributed to persistent upwelling resulting in the tapping of water from deeper subsurface layers. Such high inputs of $[SiO_2]$ relative to $[NO_3^-]$ should favour diatom production relative to the production of other non-siliceous algae in the Gulf of Tehuatepec, which is consistent with elevated opal burial and high Si:C and Si:N ratios in Holocene sediments. Further, the increase in Si:C and Si:N occur after ~11,000 years in the Gulf of Tehuantepec core (Fig. 5) when the ITCZ was established in its northernmost position (Haug et al., 2001), which could be also a factor in the establishment of the modern cyclonic circulation in the Gulf of Tehuantepec favouring the supply of waters with relatively elevated levels of silicic acid in the mid- to late Holocene.

4. Summary and implications

Our study explains the variable glacial–interglacial pattern exhibited by opal records in the eastern Pacific. The silicic acid leakage hypothesis, as originally proposed, envisioned a glacial redistribution of $Si(OH)_4$ from the Southern Ocean to the low latitudes causing an uniform increase in opal production during glacial periods (Brzezinski et al., 2002). However, changes in opal records are not uniform in the eastern Pacific. The eastern equatorial Pacific (EEP) showed lower glacial opal production and fluxes (Higginson and Altabet, 2004; Bradtmiller et al., 2006; Kienast et al., 2006; Richaud et al., 2007) whereas it increased in the coastal upwelling areas of the ETNP and off Peru and Chile (24°S and 33°S) (Mohtadi and Hebbeln, 2004). This study provides an explanation for this variable pattern by suggesting that the productivity response was different in the severely Fe-limited areas such as the HNLC regions compared to non-HNLC regions during glacial period. In the HNLC regions like the EEP the silicic acid usage declined during glacials, due to reduced Si:N uptake during diatom growth, as suggested by a recent study (Pichevin et al., 2009) and therefore did not witness a net increase in opal fluxes. Adjoining areas such as the ETNP (this study) and the Peru-Chile margin (Mohtadi and Hebbeln, 2004) benefited from the export of the excess silicic acid created in the glacial EEP and record increased opal contents and fluxes at that time. If this glacial redistribution of $Si(OH)_4$ and the consequent increase in siliceous production documented here in the ETNP margins were to occur more widely, this could have increased the rain rate ratios in the low-latitude Pacific ocean contributing to lower the pCO_2 of this period. Currently, the records are too sparse in coverage to fully evaluate this scenario.

More broadly, our study illustrates the complexity in interpreting opal records. Traditionally, variability in opal records were linked to changes in productivity and upwelling history (e.g. Charles et al., 1991; Rathburn et al., 2001). We suggest that at least three additional factors can affect opal records. First, changes in Si:N uptake ratios of diatoms in response to variability in Fe-availability in HNLC regions, as illustrated by the EEP where opal fluxes were reduced due to lower Si:N uptake ratios by growing diatoms under conditions of increased Fe-availability. Second, changes in the supply and availability of silicic acid relative to other macronutrients can influence diatom versus non-siliceous production in Si limited areas. Such additional Si supply explains the increase in opal fluxes in the ETNP margins during glacial periods, despite the relative decline in upwelling during this period (Ganeshram and Pedersen, 1998; Hendy and Kennett, 2000; Hendy et al., 2004; Ortiz et al., 2004). Finally, opal burial can also vary with the nature of upwelling waters from various depths resulting in changes in the levels of $Si(OH)_4$ relative to nitrate responding to local climatological factors as discussed in the case of the Gulf of Tehuantepec. All these factors need to be considered in interpreting sedimentary opal records in paleoceanographic studies.

Acknowledgments

This study was funded by a NERC standard grant and a European Science Foundation grant awarded to RSG. We are thankful to the

staff and crew of RV *Marion* Dufresne for coring support through IMAGES IV programme. EAT is grateful to the ORSAS Scholarship scheme that supported her study at the School of Geosciences, The University of Edinburgh. Support for LEP was provided by the Marie Curie Intra-European Fellowship and the Scottish Alliance for Geoscience, Environment and Society (SAGES). Radiocarbon dating was conducted through NERC RCL allocations 1132.0405 (Core MD02-2520), 1202.1006 (MD02-2524) and 1259.1007 (MD02-2519). We thank Dr. Steve Moreton (NERC RCL) for his help with radiocarbon dating and Colin Chilcott for CN analyses.

References

Ahn, J., Brook, E.J., 2008. Atmospheric CO_2 and climate on millennial time scales during the last glacial period. Science 322, 83–85.

Archer, D., Maierreimer, E., 1994. Effect of deep-sea sedimentary Calcite preservation on atmospheric CO_2 concentration. Nature 367, 260–263.

Archer, D., Winguth, A., Lea, D., Mahowald, N., 2000a. What caused the glacial/interglacial atmospheric pCO(2) cycles? Reviews of Geophysics 38, 159–189.

Archer, D.E., Eshel, G., Winguth, A., Broecker, W., Pierrehumbert, R., Tobis, M., Jacob, R., 2000b. Atmospheric pCO(2) sensitivity to the biological pump in the ocean. Global Biogeochemical Cycles 14, 1219–1230.

Bard, E., Rostek, F., Menot-Combes, G., 2004. Radiocarbon calibration beyond 20,000 C-14 yr BP by means of planktonic foraminifera of the Iberian Margin. Quaternary Research 61, 204–214.

Barron, J.A., Bukry, D., Bischoff, J.L., 2004. High resolution paleoceanography of the Guaymas Basin, Gulf of California, during the past 15000 years. Marine Micropaleontology 50, 185–207.

Barton, E.D., Lavín, M.F., Trasviña, A., 2009. Coastal circulation and hydrography in the Gulf of Tehuantepec, Mexico, during winter. Continental Shelf Research 29, 485–500.

Beaufort, L., 2002. IMAGES VIII MONA Cruise Report, Institut Polaire Francais Paul-Émile Victor (IPEV), les rapports de campagnes à la mer OCE/2002/03, PANGAEA. http://www.images-pages.org/ftp/pub/MONA/MONA_cruise_report.pdf 452.

Berger, W.H., Wefer, G., 1991. Productivity of the glacial ocean - Discussion of the iron hypothesis. Limnology and Oceanography 36, 1899–1918.

Boyle, E., 1998. Pumping iron makes thinner diatoms. Nature 393, 733–734.

Bradtmiller, L.I., Anderson, R.F., Fleisher, M.Q., Burckle, L.H., 2006. Diatom productivity in the equatorial Pacific Ocean from the last glacial period to the present: a test of the silicic acid leakage hypothesis. Paleoceanography 21. doi:10.1029/2006PA001282.

Bradtmiller, L.I., Anderson, R.F., Fleisher, M.Q., Burckle, L.H., 2009. Comparing glacial and Holocene opal fluxes in the Pacific sector of the Southern Ocean. Paleoceanography 24 PA2214.

Broecker, W.S., Bond, G.C., Klas, M., Clark, E., McManus, J., 1992. Origin of the northern Atlantic Heinrich events. Climate Dynamics 6, 265–273.

Bruland, K.W., Rue, E.L., Smith, G.J., 2001. Iron and macronutrients in California coastal upwelling regimes: implications for diatom Blooms. Limnology and Oceanography 46, 1661–1674.

Brzezinski, M.A., Nelson, D.M., 1996. Chronic substrate limitation of silicic acid uptake rates in the western Sargasso Sea. Deep-Sea Research Part Ii-Topical Studies in Oceanography 43, 437–453.

Brzezinski, M.A., Pride, C.J., Franck, V.M., Sigman, D.M., Sarmiento, J.L., Matsumoto, K., Gruber, N., Rau, G.H., Coale, K.H., 2002. A switch from Si(OH)(4) to NO3- depletion in the glacial Southern Ocean. Geophysical Research Letters 29. doi:10.1029/2001GL014349.

Brzezinski, M.A., Dickson, M.-L., Nelson, D.M., Sambrotto, R., 2003. Ratios of Si, C and N uptake by microplankton in the southern ocean. Deep Sea Research Part II: Topical Studies in Oceanography 50, 619–633.

Brzezinski, M.A., Dumousseaud, C., Krause, J.W., Measures, C.I., Nelson, D.M., 2008. Iron and silicic acid concentrations together regulate Si uptake in the equatorial Pacific Ocean. Limnology and Oceanography 53, 875–889.

Charles, C.D., Froehlich, P.N., Zibello, M.A., Mortlock, R.A., Morely, J.J., 1991. Biogenic opal in southern ocean sediment over the past 450,000 years: implications for surface water chemistry and circulation. Paleoceanography 6, 697–728.

Chase, Z., Anderson, R.F., Fleisher, M.Q., Kubik, P.W., 2003. Accumulation of biogenic and lithogenic material in the Pacific sector of the Southern Ocean during the past 40,000 years. Deep Sea Research Part II: Topical Studies in Oceanography 50, 799–832.

DeMaster, D.J., 2002. The accumulation and cycling of biogenic silica in the Southern Ocean: revisiting the marine silica budget. Deep-Sea Research Part II-Topical Studies in Oceanography 49, 3155–3167.

Dezileau, L., Reyss, J.L., Lemoine, F., 2003. Late Quaternary changes in biogenic opal fluxes in the Southern Indian Ocean. Marine Geology 202, 143–158.

Diekmann, B., 2007. Sedimentary patterns in the late quaternary southern ocean. Deep Sea Research Part II: Topical Studies in Oceanography 54, 2350–2366.

Douglas, R., Gonzalez-Yajimovich, O., Ledesma-Vazquez, J., Staines-Urias, F., 2007. Climate forcing, primary production and the distribution of Holocene biogenic sediments in the Gulf of California. Quaternary Science Reviews 26, 115–129.

Dugdale, R.C., Wischmeyer, A.G., Wilkerson, F.P., Barber, R.T., Chai, F., Jiang, M.S., Peng, T.H., 2002. Meridional asymmetry of source nutrients to the equatorial Pacific upwelling ecosystem and its potential impact on ocean-atmosphere CO_2 flux; a data and modeling approach. Deep-Sea Research Part Ii-Topical Studies in Oceanography 49, 2513–2531.

Dymond, J., Lyle, M., 1985. Flux comparisons between sediments and sediment traps in the eastern tropical Pacific: implications for atmospheric CO_2 variations during the Pleistocene. Limnology and Oceanography 30, 699–712.

Egge, J.K., Aksnes, D.L., 1992. Silicate as Regulating nutrient in phytoplankton Competition. Marine Ecology-Progress Series 83, 281–289.

Farber-Lorda, J., Lavín, M.F., Guerrero-Ruiz, M.A., 2004. Effects of wind forcing on the trophic conditions, zooplankton biomass and krill biochemical composition in the Gulf of Tehuantepec. Deep Sea Research Part II: Topical Studies in Oceanography 51, 601–614.

Fiedler, P.C., Talley, L.D., 2006. Hydrography of the eastern tropical Pacific: a review. Progress in Oceanography 69, 143–180.

Firme, G.F., Rue, E.L., Weeks, D.A., Bruland, K.W., Hutchins, D.A., 2003. Spatial and temporal variability in phytoplankton iron limitation along the California coast and consequences for Si, N, and C biogeochemistry. Global Biogeochemcal Cycles 17.

Franck, V.M., Brzezinski, M.A., Coale, K.H., Nelson, D.M., 2000. Iron and silicic acid concentrations regulate Si uptake north and south of the Polar Frontal zone in the Pacific sector of the southern ocean. Deep Sea Research Part II: Topical Studies in Oceanography 47, 3315–3338.

Francois, R., Altabet, M.A., Yu, E.F., 1997. Contribution of Southern Ocean surface-water stratification to low atmospheric CO2 concentrations during the last glacial period. Nature 389, 929–935.

Frank, M., Gersonde, R., van der Loeff, M.R., Bohrmann, G., Nürnberg, C.C., Kubik, P.W., Suter, M., Mangini, A., 2000a. Similar glacial and interglacial export bioproductivity in the Atlantic sector of the southern Ocean: Multiproxy evidence and implications for glacial atmospheric CO_2. Paleoceanography 15, 642–658.

Frank, M.V., Brzezinski, M.A., Coale, K.H., Nelson, D.M., 2000b. Iron and silicic acid concentrations regulate Si uptake north of the Polar Frontal zone in the Pacific sector of the southern ocean. Deep Sea Research Part II: Topical Studies in Oceanography 47, 3315–3338.

Ganeshram, R.S., 2002. Global change - Oceanic action at a distance. Nature 419, 123–125.

Ganeshram, R.S., Pedersen, T.F., 1998. Glacial-interglacial variability in upwelling and bioproductivity off NW Mexico: implications for quaternary paleoclimate. Paleoceanography 13, 634–645.

Ganeshram, R.S., Pedersen, T.F., Calvert, S.E., Murray, J.W., 1995. Large changes in oceanic nutrient Inventories from glacial to interglacial periods. Nature 376, 755–758.

Ganeshram, R.S., Calvert, S.E., Pedersen, T.F., Cowie, G.L., 1999. Factors controlling the burial of organic carbon in laminated and bioturbated sediments off NW Mexico: implications for hydrocarbon preservation. Geochimica Et Cosmochimica Acta 63, 1723–1734.

Haug, G.H., Hughen, K.A., Sigman, D.M., Peterson, L.C., Röhl, U., 2001. Southward Migration of the Intertropical Convergence zone through the Holocene. Science 293, 1304–1308.

Hendy, I.L., Kennett, J.P., 2000. Dansgaard-Oeschger cycles and the California current System: planktonic foraminiferal response to rapid climate change in Santa Barbara basin, Ocean Drilling Program hole 893A. Paleoceanography 15, 30–42.

Hendy, I.L., Kennett, J.P., Roark, E.B., Ingram, B.L., 2002. Apparent synchroneity of submillennial scale climate events between Greenland and Santa Barbara Basin, California from 30-10 ka. Quaternary Science Reviews 21, 1167–1184.

Hendy, I.L., Pedersen, T.F., Kennett, J.P., Tada, R., 2004. Intermittent existence of a southern Californian upwelling cell during submillennial climate change of the last 60 kyr. Paleoceanography 19. doi:10.1029/2003PA000965.

Higginson, M.J., Altabet, M.A., 2004. Initial test of the silicic acid leakage hypothesis using sedimentary biomarkers. Geophysical Research Letters 31. doi:10.1029/2004GL020511.

Hutchins, D.A., Bruland, K.W., 1998. Iron-limited diatom growth and Si: N uptake ratios in a coastal upwelling regime. Nature 393, 561–564.

Kessler, W.S., 2006. The Circulation of the Eastern Tropical Pacific: A Review, Progress in Oceanography 69, 181–217.

Kienast, S.S., Kienast, M., Jaccard, S., Calvert, S.E., Francois, R., 2006. Testing the silica leakage hypothesis with sedimentary opal records from the eastern equatorial Pacific over the last 150 kyrs. Geophysical Research Letters 33. doi:10.1029/2006GL026651.

Lefevre, N., Watson, A.J., 1999. Modelling the geochemical cycle of iron in the oceans and its impact on atmospheric CO_2 concentrations. Global Biogeochem. Cycles 13, 727–736.

Levitus, S., Burgett, R., Boyer, T.P., 1994. World Ocean Atlas 1994 3: Nutrients.

Leynaert, A., Bucciarelli, E., Claquin, P., Dugdale, R.C., Martin-Jézéquel, V., Pondaven, P., Ragueneau, O., 2004. Effect of iron Deficiency on diatom cell Size and silicic acid uptake Kinetics. Limnology and Oceanography 49, 1134–1143.

Marchetti, A., Cassar, N., 2009. Diatom elemental and morphological changes in response to iron limitation: a brief review with potential paleoceanographic applications. Geobiology 7, 419–431.

Marchetti, A., Varela, D.E., Lance, V.P., Johnson, Z., Palmucci, M., Giordano, M., Virginia, A.E., 2010. Iron and silicic acid effects on phytoplankton productivity, diversity, and chemical composition in the central equatorial Pacific Ocean. Limnology and Oceanography 55, 11–29.

Martin, J.H., Fitzwater, S.E., Gordon, R.M., 1990. Iron Deficiency limits phytoplankton growth in Antarctic waters. Global Biogeochemical Cycles 4, 5–12.

Matsumoto, K., Sarmiento, J.L., 2008. A corollary to the silicic acid leakage hypothesis. Paleoceanography 23 PA2203.

Matsumoto, K., Sarmiento, J.L., Brzezinski, M.A., 2002. Silicic acid leakage from the Southern Ocean: a possible explanation for glacial atmospheric pCO(2). Global Biogeochemical Cycles 16. doi:10.1029/2001GB001442.
McGee, D., Marcantonio, F., Lynch-Stieglitz, J., 2007. Deglacial changes in dust flux in the eastern equatorial Pacific. Earth and Planetary Science Letters 257, 215–230.
Mohtadi, M., Hebbeln, D., 2004. Mechanisms and variations of the paleoproductivity off northern Chile (24 degrees S-33 degrees S) during the last 40,000 years. Paleoceanography 19. doi:10.1029/2004PA001003.
Monnin, E., Indermuhle, A., Dallenbach, A., Fluckiger, J., Stauffer, B., Stocker, T.F., Raynaud, D., Barnola, J.-M., 2001. Atmospheric CO_2 concentrations over the last glacial termination. Science 291, 112–114.
Moore, J.K., Doney, S.C., Lindsay, K., 2004. Upper ocean ecosystem dynamics and iron cycling in a global three-dimensional model. Global Biogeochemical Cycles 18. doi:10.1029/2004GB002220.
Mortlock, R.A., Froelich, P.N., 1989. A Simple Method for the rapid-determination of biogenic opal in Pelagic marine-Sediments. Deep-Sea Research Part A-Oceanographic Research Papers 36, 1415–1426.
Mosseri, J., QuÈguiner, B., Armand, L., Cornet-Barthaux, V., 2008. Impact of iron on silicon utilization by diatoms in the Southern Ocean: a case study of Si/N cycle decoupling in a naturally iron-enriched area. Deep Sea Research Part II: Topical Studies in Oceanography 55, 801–819.
Nelson, D.M., Brzezinski, M.A., Sigmon, D.E., Franck, V.M., 2001. A seasonal progression of Si limitation in the Pacific sector of the Southern Ocean. Deep-Sea Research Part Ii-Topical Studies in Oceanography 48, 3973–3995.
Nelson, D.M., Anderson, R.F., Barber, R.T., Brzezinski, M.A., Buesseler, K.O., Chase, Z., Collier, R.W., Dickson, M.L., Francois, R., Hiscock, M.R., Honjo, S., Marra, J., Martin, W.R., Sambrotto, R.N., Sayles, F.L., Sigmon, D.E., 2002. Vertical budgets for organic carbon and biogenic silica in the Pacific sector of the Southern Ocean, 1996–1998. Deep-Sea Research Part II-Topical Studies in Oceanography 49, 1645–1674.
Ortiz, J.D., O'Connell, S.B., DelViscio, J., Dean, W., Carriquiry, J.D., Marchitto, T., Zheng, Y., van Geen, A., 2004. Enhanced marine productivity off western North America during warm climate intervals of the past 52 ky. Geology 32, 521–524.
Pennington, J.T., Mahoney, K.L., Kuwahara, V.S., Kolber, D.D., Calienes, R., Chavez, F.P., 2006. Primary production in the eastern tropical Pacific: a review. Progress in Oceanography 69, 285–317.
Pichevin, L.E., Reynolds, B.C., Ganeshram, R.S., Cacho, I., Pena, L.D., Keefe, K., Ellam, R.M., 2009. Enhanced carbon pump inferred from relaxation of nutrient limitation in the glacial ocean. Nature 459, 1114–1117.
Pichevin, L.E., Ganeshram, R.S., Francavilla, S., Arellano-Torres, E., Pedersen, T.F., Beaufort, L., 2010. Inter-hemispheric leakage of isotopically heavy nitrate in the Eastern Tropical Pacific during the last glacial period. Paleoceanography 25. doi:10.1029/2009PA001754.
Ragueneau, O., Treguer, P., Leynaert, A., Anderson, R.F., Brzezinski, M.A., DeMaster, D.J., Dugdale, R.C., Dymond, J., Fischer, G., Francois, R., Heinze, C., Maier-Reimer, E., Martin-Jezequel, V., Nelson, D.M., Queguiner, B., 2000. A review of the Si cycle in the modem ocean: recent progress and missing gaps in the application of biogenic opal as a paleoproductivity proxy. Global and Planetary Change 26, 317–365.
Rathburn, A.E., Perez, M.E., Lange, C.B., 2001. Benthicepelagic coupling in the Southern California Bight: relationships between sinking organic material, diatoms, benthic foraminifera. Marine Micropaleontology 43, 261–271.
Reimer, P.J., Reimer, R.W., 2001. A marine reservoir correction database and on-line interface. Radiocarbon 43, 461–463. supplemental material URL. http://www.calib.org.
Richaud, M., Loubere, P., Pichat, S., Francois, R., 2007. Changes in opal flux and the rain ratio during the last 50,000 years in the equatorial Pacific. Deep-Sea Research Part Ii-Topical Studies in Oceanography 54, 762–771.
Ridgwell, A.J., Watson, A.J., Archer, D.E., 2002. Modeling the response of the oceanic Si inventory to perturbation, and consequences for atmospheric CO_2. Global Biogeochemical Cycles 16.
Sigman, D.M., Boyle, E.A., 2000. Glacial/interglacial variations in atmospheric carbon dioxide. Nature 407, 859–869.
Stuiver, M., Reimer, P.J., Reimer, R.W., 2005. CALIB 5.0 [WWW program and documentation].
Takeda, S., 1998. Influence of iron availability on nutrient consumption ratio of diatoms in oceanic waters. Nature 393, 774–777.
Takeda, S., Yoshie, N., Boyd, P.W., Yamanaka, Y., 2006. Modeling studies investigating the causes of preferential depletion of silicic acid relative to nitrate during SERIES, a mesoscale iron enrichment in the NE subarctic Pacific. Deep Sea Research Part II: Topical Studies in Oceanography 53, 2297–2326.
Toggweiler, J.R., Carson, S., 1995. What are upwelling systems contributing to the ocean's carbon and nutrient budgets. Upwelling in the Ocean 18, 337–360.
Trasviña, A., Barton, E.D., 2008. Summer circulation in the Mexican tropical Pacific. Deep Sea Research Part I: Oceanographic Research Papers 55, 587–607.
Trasviña, A., Barton, E.D., Brown, J., Velez, H.S., Kosro, P.M., Smith, R.L., 1995. Offshore wind forcing in the Gulf of Tehuantepec, Mexico - the Asymmetric circulation. Journal of Geophysical Research-Oceans 100, 20649–20663.
Tsuchiya, M., Talley, L.D., 1996. Water-property distributions along an eastern Pacific hydrographic section at 135W. Journal of Marine Research 54, 541–564.
Tsuchiya, M., Talley, L.D., 1998. A Pacific hydrographic section at 88 degrees W: water-property distribution. Journal of Geophysical Research-Oceans 103, 12899–12918.
Watson, A.J., Bakker, D.C.E., Ridgwell, A.J., Boyd, P.W., Law, C.S., 2000. Effect of iron supply on Southern Ocean CO_2 uptake and implications for glacial atmospheric CO_2. Nature 407, 730–733.
Winckler, G., Anderson, R.F., Fleisher, M.Q., McGee, D., Mahowald, N., 2008. Covariant glacial-interglacial dust fluxes in the equatorial Pacific and Antarctica. Science 320, 93–96.
Wong, C.S., Johnson, W.K., Sutherland, N., Nishioka, J., Timothy, D.A., Robert, M., Takeda, S., 2006. Iron speciation and dynamics during SERIES, a mesoscale iron enrichment experiment in the NE Pacific. Deep Sea Research Part II: Topical Studies in Oceanography 53, 2075–2094.
Wyrtki, K., 1966. Intermediate waters of Pacific ocean. Limnology and Oceanography 11, 313–317.